ADVANCED ENERGY MATERIALS
www.advenergymat.de

Fully Packaged Self-Powered Triboelectric Pressure Sensor Using Hemispheres-Array

Keun Young Lee, Hong-Joon Yoon, Tao Jiang, Xiaonan Wen, Wanchul Seung, Sang-Woo Kim, and Zhong Lin Wang**

Integrating individual devices into micro/nanosystems is essential for the Internet of Things (IoT), including electronics, sensors, network, and software, which enables these systems to do sensing, communicating, controlling, and responding.[1–3] Concerning this technological trend, sustainable power sources to operate these systems is hugely demanded because conventional power source until now, for example battery, have some drawbacks such as limited lifetime and difficulties of maintenance as well as environmental issues.[4] Among sustainable power sources, triboelectric nanogenerators (TENGs) have been successfully demonstrated as powerful means of harvesting mechanical energy, which is universally available in ambient environment at anytime and anywhere.[5–25]

In the triboelectric process, once material's surface becomes electrically charged after periodic contact-separation[8–10] or in-plane sliding/rotating[11–13] with a different material; the triboelectric charges produce a potential that drives free electrons in the two electrodes to flow in the external circuit. TENGs in contact-separation mode require a gap for separating the two materials so that TENG can convert periodic triggering into periodic contact-separation between the tribo-layers for generating an AC current.[14] However, the required gap and the air exchange during mechanical triggering make the packaging of the TENG rather challenging especially for applications in severe environment such as in dusty or moisture atmosphere.[17–21] It is known that moisture can largely eliminate surface triboelectric charges and reduce the output.[22–24] Thus, an embeddable and packaged design of TENGs is necessary to be sustainable power source in harsh and dangerous environment.

K. Y. Lee, X. Wen, Z. L. Wang
School of Material Science and Engineering
Georgia Institute of Technology
Atlanta, GA 30332-0245, USA
E-mail: zlwang@gatech.edu
K. Y. Lee, H.-J. Yoon, W. Seung, S.-W. Kim
School of Advanced Materials Science and Engineering
Sungkyunkwan University (SKKU)
Suwon 440-746, Republic of Korea
E-mail: kimsw1@skku.edu
T. Jiang, Z. L. Wang
Beijing Institute of Nanoenergy and Nanosystems
Chinese Academy of Sciences
Beijing 100083, China
S.-W. Kim
SKKU Advanced Institute of Nanotechnology (SAINT)
Center for Human Interface Nanotechnology (HINT)
Sungkyunkwan University
Suwon 440-746, Republic of Korea

DOI: 10.1002/aenm.201502566

Here, we demonstrate a newly designed fully packaged TENG based on hemispheres-array-structure, whose structure is firmly built in enclosed and packaged system without any spacer. The hemispheres-array-structured TENGs (H-TENGs) exhibit high mechanical durability, excellent robustness behavior, and high elastic property. Different diameters of H-TENGs were fabricated and their output performances were measured under various vertical compressive forces. We demonstrated that fabricated H-TENG can be utilized as an active self-powered sensor array to map the distribution of foot produced pressure, which is designed to enhance human-electronics interaction.

A schematic illustration of the H-TENGs based on elastic hemispheres-array-structured film is shown in **Figure 1**. The H-TENG mainly consists of five layers: a layer of polydimethylsiloxane (PDMS) hemispheres-array-structure with copper (Cu)-deposited on top, which acts as the elastic triboelectric material and the bottom electrode; a PTFE (polytetrafluoroethylene) film that has an opposite triboelectric polarity than Cu followed by the deposition of an Cu layer electrode as the top electrode; the entire structure is sandwiched between two acrylic substrates as shown in Figure 1a. The device can be packaged with not only rigid one, but also elastic materials such as PDMS, which results in a wide range of applicable properties under various mechanical strains induced by tensile and bending motions. Figure S2 in the Supporting Information shows that packaged H-TENG with elastic PDMS is able to be both stretchable and flexible. Figure 1b displays a corresponding photograph of the H-TENG. The hemispheres-array-structured film was fabricated by replication process (See the Experimental Section and Figure S1 in the Supporting Information for fabrication details).[25–31] The morphologies of hemispheres-array-structured film were further characterized by field emission-scanning electron microscopy as shown in Figure 1c. It can be seen that the hemispheres-array-structured film has been uniformly formed. The corresponding morphologies of the hemispheres-array-structured film fabricated with different diameters of 90, 600 μm, and 3 mm are shown in Figure S3 in the Supporting Information.

The working mechanism of the fabricated H-TENG is schematically presented in **Figure 2**a and Figure S4 in the Supporting Information. At the initial state, the top area of Cu-deposited hemispheres-array-structured film created a point of contact with PTFE film, where there is no charge transfer, which results in no electric potential. When a compressive force is applied to the H-TENG, the Cu-deposited hemispheres-array-structured film starts to be deformed and dimensional flat contact area is created with PTFE film accordingly. The contact area between the hemispheres-array-structured film and PTFE film depends on the applied compressive force. Positive triboelectric

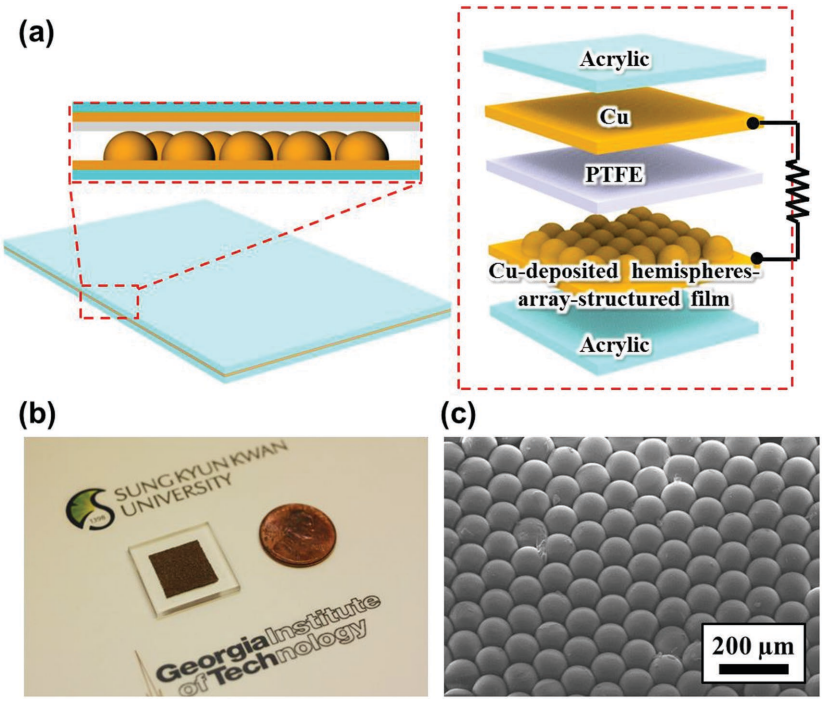

Figure 1. Schematic description of the H-TENGs. a) Illustration of ultrathin H-TENGs and its stacked structure and packaged module. b) Real visual image of H-TENGs. c) FE-SEM images of the hemispheres-array-structured film.

charges on the surface of hemispheres-array-structured film, and negative triboelectric charges on the PTFE film are created by triboelectric effect. At this stage, H-TENG remains in electrostatic equilibrium state due to negligible dipole moment. As we released H-TENG, strong dipole moment was formed due to electrostatic effect, which results in an electrical potential difference between the bottom and top electrodes. Because the Cu-deposited hemispheres-array-structured film has a higher potential than the top Al electrode, electrons started to flow from the top electrode to the bottom electrode through the external circuit to neutralize the negative triboelectric charges in the top electrode, which results in electric signal observed from the H-TENG.

To understand the working mechanism, the COMSOL software was used to investigate the electric potential distribution in the H-TENG (3 mm diameter hemispheres-array-structured film) as a function of the deformation depth (Δh) of hemispheres-array-structured film by compressive force (Figure 2 b, c). It was found that the electric potential difference between the two electrodes decreases as the deformation depth increases. We further calculated the open-circuit voltage (V_{OC}) in the H-TENGs based on 90, 600 μm, and 3 mm diameter of hemispheres-array-structured film as a function of the deformation ratio ($\Delta h/h$) as shown in Figure 2d. As the diameter of hemispheres decreases, the V_{OC} also decreases. The reason is that the triboelectric output performance is determined by the separation distance between two opposite tribo-materials during periodic contact-separation.[32] The H-TENGs with a smaller diameter of hemispheres show a shorter separation distance, therefore they exhibit relatively lower output performance. According to theoretical studies the induced V_{OC} is defined by the following descriptions.

When there is no deformation ($\Delta h = 0$), if we define the average separation distance as d, the total capacitance can be given by

$$C(0) = \frac{\varepsilon_0 S}{d} \quad (1)$$

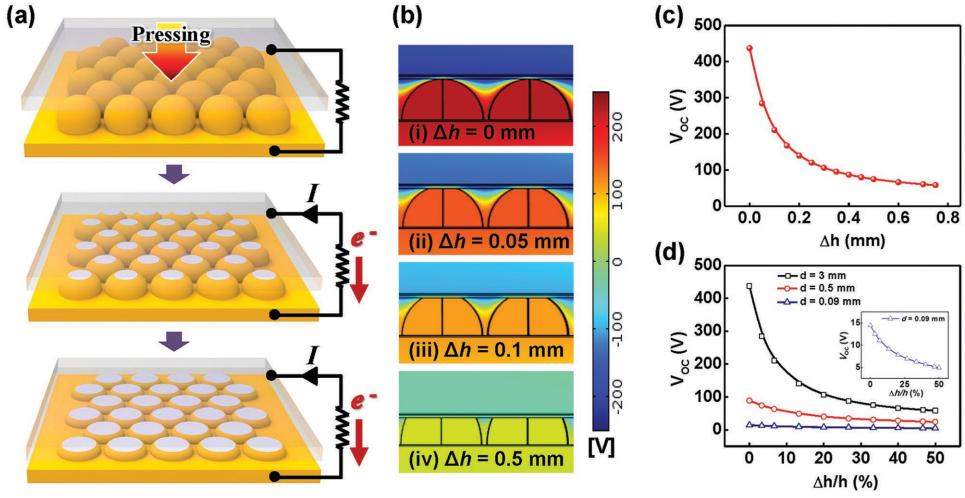

Figure 2. a) Sequential diagrams of H-TENGs at compressive force. b) Numerically calculated potential distribution on surface of hemispheres with different deformation depths. c) Plotted open-circuit voltage (V_{oc}) values of H-TENGs as the function of deformation depth (Δh) corresponding to (b). d) Plots of open-circuit voltage (V_{oc}) of H-TENGs with various diameters of hemisphere as the function of deformation ratio ($\Delta h/h$) (inset: Enlarged open-circuit voltage (V_{oc}) values of H-TENG based on 0.09 mm of diameter of hemisphere).

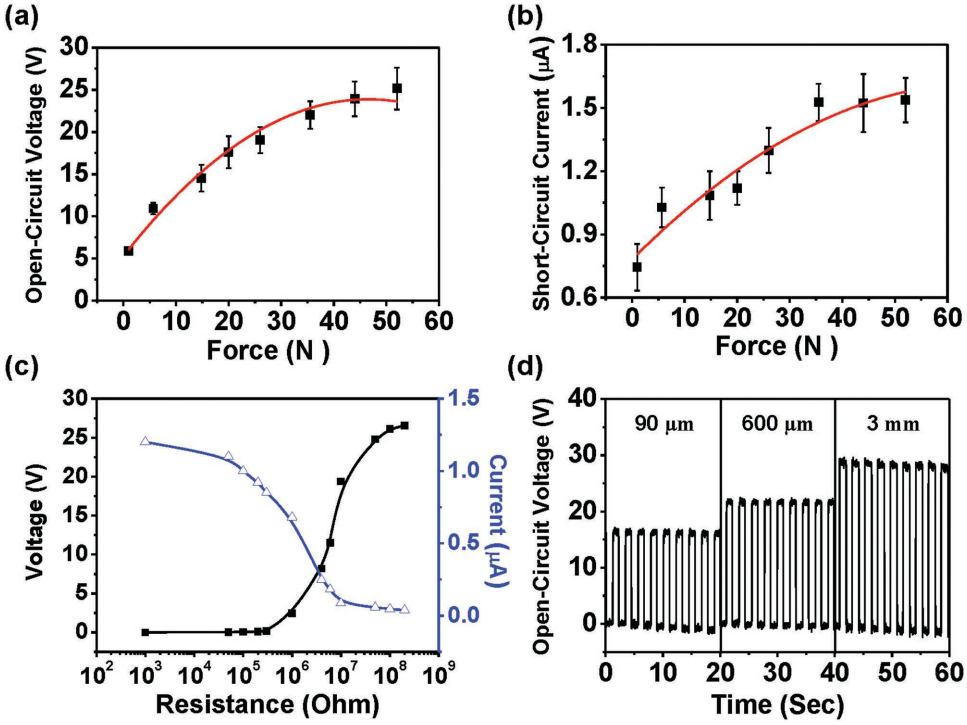

Figure 3. Electrical output performance of the H-TENGs. a) Open-circuit voltage (V_{oc}) and b) short-circuit current (I_{sc}) of the H-TENG (3 mm) depending on different compressive force. c) Optimum output power derived from both output voltage and current at different internal resistances. d) Varied open-circuit voltage (V_{oc}) of H-TENGs with different diameter of hemispheres.

where ε_0 is the permittivity of vacuum, S is the tribo-surface area of PTFE film. When imposed a deformation depth Δh, the average separation distance becomes d-Δh, and the capacitance is given by

$$C(\Delta h) = \frac{\varepsilon_0 S}{d - \Delta h} \tag{2}$$

Thus, as Δh increased the capacitance of H-TENG increases, and the *Voc* decrease as derived by following equation

$$V_{OC}(\Delta h) = \frac{\sigma(d - \Delta h)}{\varepsilon_0} \tag{3}$$

Figures 3a,b present the output voltage and current from the H-TENG (3 mm diameter hemispheres-array-structured film) as a function of the force applied under vertical compression from a mechanical force stimulator. The output voltage and current are increased upon compressive force due to enlarged contact area. (Their raw data are given in Figure S5 in the Supporting Information). In Figure 3c, to derive optimum output power of H-TENG, output voltage, and current were measured at various external resistances ranging from 1 KΩ to 1 GΩ, which results in 2.45 μW of output power generated at 3 MΩ. We further measured the output voltage for all cases of diameters of hemispheres ranging from 90 to 600 μm under the same compressive force. As the diameter of hemispheres decreases to 90 μm, the output voltage decreases significantly as described in Figure 3d, which is the same as the theoretical result in Figure 2d.

Output performance of H-TENG is determined by two dominant effects. One is triboelectric effect that is created by periodic contacts between two materials that differ in polarity of triboelectricity. Another one is the electrostatic effect that is made by the potential difference between two charged materials when those are mechanically separated. Recently there have been numerous reports demonstrating that mechanical or chemical treatments are applied to enhance surface area of TENGs for efficient contact or the amount of charges on surface to be generated and transferred upon periodic triboelectric effect. In case of H-TENGs, hemispheres-array-structure themselves participate in contact-separation cycles as well as enhance contact area due to the special curved geometrical structure. On top of that, because H-TENGs are fully packaged, their whole thickness of the device is determined by the diameter of the hemispheres-array-structure. And thus, the bigger diameter of hemispheres-array-structured film based device is apt to be even more deformed than the smaller one at the same deformation ratio. In other words, in aspect of electrostatic effect, the bigger diameter of hemispheres-array-structured film based device has large displacement between two opposite triboelectric materials, which induce high electric potential. To be summarized, the deformation depth (Δh) predominantly impacts on output performance of H-TENGs more than any other factors such as tribo-charges or density.

Besides, since the hemispheres are quite elastic, they function as a spring to keep the two opposite materials separate. Compared to conventional spring-assisted TENGs for the separation of both materials, triboelectric material itself plays as a spring due to its elasticity. In addition, hemispheres have high

durable and robust properties, and so it is suitable and realizable for H-TENGs to be used for long-term application with constant performance as shown in Figure S6 in the Supporting Information, demonstrating the device performed with great stability under approximately 5000 times for 600 s. Even after multiple pushing cycles, there seems very little degradation on surface morphologies of hemispheres-array-structured film as characterized by a field emission-scanning electron microscopy shown in Figure S7 in the Supporting Information. We concluded that enhanced output performance and architectural advantages of H-TENGs are determined by physical properties of hemispheres including diameter, deformed magnitude, and elasticity. In addition, the diameter of hemisphere would be also suited on applications because different space may exist with various applications.

To demonstrate the application of the H-TENGs as an effective power source to operate in severe environment such as dust or moisture atmosphere, the H-TENG fully packaged by PDMS was measured under water and measured under ambient air condition for comparison in **Figure 4**a,b, respectively. It is clearly seen that the output performance of the perfectly packaged H-TENG is very stable, and there is no significant differences. This result shows that the output performance of H-TENG is not significantly influenced by external condition, and so it is applicable as power source in severe environment even under water. Furthermore, we demonstrated the self-powered pressure mapping sensor for detecting applied multiple forces in real-time. As shown in Figure 4c, the H-TENGs with an active area of 1 cm × 1 cm were arrayed on matrix patterned electrodes and the different pressures from a foot modeled by 3D printer can be identified by measuring the distribution of strain by H-TENGs (The foot model is well described in detail in Figure S8 in the Supporting Information). The peeled off device is visually illustrated as an inset for better understanding of its structure. Figure 4d shows a two-dimensional contour plot that reconstructs applied forces of each array and is mapping overall potential gained from the foot. The resolution of the present pressure sensor system depends on a number of parameters such as the density of arrays, diameter of hemisphere, and the distance between arrays. For the given modeled foot, magnitude of all gained pressure to each unit array is indicated as the corresponding pressure intensities on the array, which is agreed with characterized results (measured raw output data set is given in Figure S9 in the Supporting Information). Since this system can collect pressures very accurately, all forms of both planar and vertical forces derived from human motions such as standing, walking, running, and sliding can be detectable at low cost with simple fabrication process. H-TENGs can function well and stable as both power source and sensors for example in wearable electronics regardless of the atmosphere, dust, and even sweat. Therefore, H-TENGs based pressure sensor demonstrates the potential to apply on health care monitoring system to collect pressure information regarding to related symptoms and sensor networks in between human and electronics interfaces, and even being an implantable device is realizable owing to its packaged, ultrathin, and flexible design.

In summary, we have demonstrated ultrathin and fully packaged H-TENGs with a completely stable electrical output performance under harsh environmental condition such as underwater. The H-TENGs composed of mainly hemispheres-array-structured film in micro/nanoscale thickness, and various diameters of hemispheres based devices were fabricated. Since the hemispheres-array-structure function as a spring to keep both top and bottom materials separate, no-spacer TENGs are successfully designed. Influences of various external compressive forces and diameters of hemisphere dependencies on

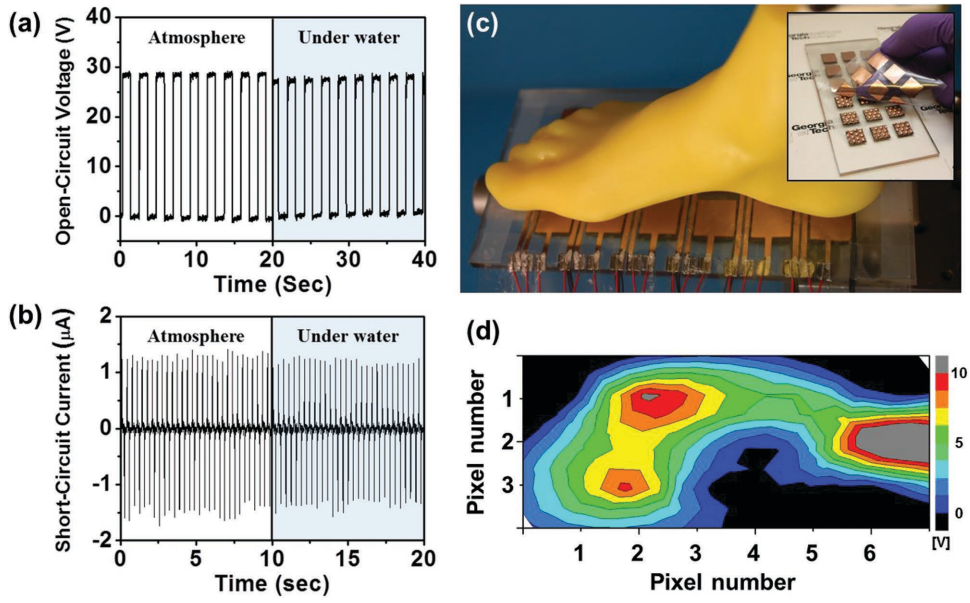

Figure 4. a) Stable open-circuit voltage (V_{oc}) and b) short-circuit current (I_{sc}) of fully packaged H-TENGs with elastomer under water condition compared to that under ambient atmosphere. c) Real visual demonstration of self-powered pressure sensor arrays (6 × 3; 1 cm × 1 cm of dimension for each unit cell) for detecting a modeled foot pressure (inset: visually illustrated peeled off device) and (d) two dimensional contour plot mapping overall potential from the object.

output performance were studied experimentally and theoretically. Both studies obtained the same result that the electrical output performance of the H-TENGs increases with an increase in the diameter of hemispheres, which is attributed to the fact that the diameter is equivalent to the separation distance between the tribo-layers. We also successfully achieved a self-powered pressure mapping sensor based on H-TENGs.

Experimental Section

Fabrication of the Hemispheres-Array-Structured Films: The replication process is schematically depicted in Figure S1 in the Supporting Information. First, oxygen plasma treatment was conducted onto a SiO_2/Si substrate for enhancing hydrophilicity and cleaning the surface. Then, polystyrene (PS) spheres with diameters of 90, 600 μm, and 3 mm (Polysciences, Inc.) was coated onto the SiO_2/Si substrate to fabricate the PS template consisting of a monolayer of PS spheres. Polydimethylsiloxane (PDMS) (Sylgard 184, Dow Corning) solution was poured onto the periodically arranged PS spheres, and allowed to solidify into an oven at 80 °C. This template was used for the first replica molding process, which led to the formation of a PDMS template with highly ordered nanopatterns on its top surface, the PDMS template was detached from the SiO2/Si substrate, and soaked in toluene for 24 h in order to remove the PS spheres. Next, a Cu film was sputtered onto the top surface of the PDMS mold. Then, another replica molding process was performed to replicate the PDMS template. Finally, the cured PDMS mold was peeled off from the PDMS template and the replicated PDMS mold was obtained.

Fabrication of the H-TENGs: A H-TENG is composed two parts. First, a hemispheres-array-structured film was attached on acrylic by double side tape to serve as bottom substrate, and then a layer of copper (Cu) (≈200 nm) was deposited using the physical vapor deposition (PVD) method which acted triboelectric material as well as the bottom electrode. On the other part, 150 μm thick PTFE film, deposited aluminum (Al) electrode on opposite side as the top electrode, were attached on acrylic attached on acrylic as top substrate. The two parts were sealed by PDMS.

Characterization: The surface morphology of the hemispheres-array-structured films was characterized by a field emission scanning electron microscope (Hitachi SU8010), and optical microscope (Nikon Eclipse Ti). For the measurement of the electric output of the H-TENGs, an external force was applied by a commercial linear mechanical motor. The open-circuit voltage was measured by using a Keithley Model 6514 system electrometer, while the short circuit current was measured by using an SR570 low-noise current amplifier (Stanford Research System). The foot was modeled by a 3D printer, Master Plus J (CARIMA).

Supporting Information

Supporting Information is available from the Wiley Online Library or from the author.

Acknowledgements

This work was financially supported by U.S. Department of Energy, Office of Basic Energy Sciences (Award DE-FG02-07ER46394), the National Science Foundation (DMR-1505319), and by Basic Science Research Program (2009-0083540) through the National Research Foundation (NRF) of Korea Grant funded by the Ministry of Science, ICT & Future Planning.

Received: December 27, 2015
Revised: March 2, 2016
Published online:

[1] K. Ashton, *RFiD J.* **2009**, *22*, 97.
[2] H. Sundmaeker, P. Guillemin, P. Friess, S. Woelfflé, *CERP IoT* **2010**, DOI: 10.2759/26127.
[3] J. Gubbi, R. Buyya, S. Marusic, M. Palaniswami, *Future Gen. Comp. Syst.* **2013**, *29*, 1645.
[4] I. Hadjipaschalis, A. Poullikkas, V. Efthimiou, *Renew. Sustain. Energy Rev.* **2009**, *13*, 1513.
[5] Z. L. Wang, *ACS Nano* **2013**, *7*, 9533.
[6] Z. L. Wang, J. Chen, L. Lin, *Energy Environ. Sci.* **2015**, *8*, 2250.
[7] R. Hinchet, W. Seung, S.-W. Kim, *ChemSusChem* **2015**, *8*, 2327.
[8] F. R. Fan, Z. Q. Tian, Z. L. Wang, *Nano Energy* **2012**, *1*, 328.
[9] F. R. Fan, L. Lin, G. Zhu, W. Z. Wu, R. Zhang, Z. L. Wang, *Nano Lett.* **2012**, *12*, 3109.
[10] S. H. Wang, L. Lin, Z. L. Wang, *Nano Lett.* **2012**, *12*, 6339.
[11] S. H. Wang, L. Lin, Y. N. Xie, Q. S. Jing, S. M. Niu, Z. L. Wang, *Nano Lett.* **2013**, *13*, 2226.
[12] L. Lin, S. H. Wang, Y. N. Xie, Q. S. Jing, S. M. Niu, Y. F. Hu, Z. L. Wang, *Nano Lett.* **2013**, *13*, 2916.
[13] P. Bai, G. Zhu, Y Liu, J. Chen, Q. Jin, W. Yang, J. Ma, G. Zhang, Z. L. Wang, *ACS Nano* **2013**, *7*, 6361.
[14] G. Zhu, Z.-H. Lin, Q. Jing, P. Bai, C. Pan, Y. Yang, Y. Zhou, Z. L. Wang, *Nano Lett.* **2013**, *13*, 847.
[15] W. Seung, M. K. Gupta, K. Y. Lee, K.-S. Shin, J.-H. Lee, T. Y. Kim, S. Kim, J. Lin, J. H. Kim, S.-W. Kim, *ACS Nano* **2015**, *9*, 3501.
[16] S. Kim, M. K. Gupta, K. Y. Lee, A. Sohn, T. Y. Kim, K.-S. Shin, D. Kim, S. K. Kim, K. H. Lee, H.-J. Shin, D.-W. Kim, S.-W. Kim, *Adv. Mater.* **2014**, *26*, 3918.
[17] Q. Zheng, B. Shi, F. Fan, X. Wang, L. Yan, W. Yuan, S. Wang, H. Liu, Z. L. Wang, *Adv. Mater.* **2014**, *26*, 5851.
[18] Y. Su, Y. Yang, X. Zhong, H. Zhang, Z. Wu, Y. Jiang, Z. L. Wang, *ACS Appl. Mater. Interfaces* **2014**, *6*, 553.
[19] H. Zhang, Y. Yang, Y. Su, J. Chen, K. Adams, S. Lee, C. Hu, Z. L. Wang, *Adv. Funct. Mater.* **2014**, *24*, 1401.
[20] B. Shi, Q. Zheng, W. Jiang, L. Yan, X. Wang, H. Liu, Y. Yao, Z. Li, Z. L. Wang, *Adv. Mater.* **2016**, *28*, 846.
[21] H. Guo, Z. Wen, Y. Zi, M.-H. Yeh, J. Wang, L. Zhu, C. Hu, Z. L. Wang, *Adv. Energy Mater.* **2015**, DOI: 10.1002/aenm.201501593.
[22] V. Nguyen, R. Yangn, *Nano Energy* **2013**, *2*, 604.
[23] K. Y. Lee, J. Chun, J.-H. Lee, K. N. Kim, N.-R. Kang, J.-Y. Kim, M. H. Kim, K.-S. Shin, M. K. Gupta, J. M. Baik, S.-W. Kim, *Adv. Mater.* **2014**, *26*, 5037.
[24] J. Chun, J. W. Kim, W.-S. Jung, C.-Y. Kang, S.-W. Kim, Z. L. Wang, J. M. Baik, *Energy Environ. Sci.* **2015**, *8*, 3006.
[25] J. H. Lee, R. Hinchet, S. K. Kim, S. Kim, S.-W. Kim, *Energy Environ. Sci.* **2015**, *8*, 3605.
[26] J.-H. Lee, H.-J. Yoon, T. Y. Kim, M. K. Gupta, J. H. Lee, W. Seung, H. Ryu, S.-W. Kim, *Adv. Funct. Mater.* **2015**, *25*, 3203.
[27] H. Hassanin, A. Mohammadkhani, K. Jiang, *LabChip* **2012**, *12*, 4160.
[28] S. C. B. Mannsfeld, B. C-K. Tee, R. M. Stoltenberg, C. V. H-H. Chen, S. Barman, B. V. O. Muir, A. N. Sokolov, C. Reese, Z. Bao, *Nat. Mater.* **2010**, *9*, 859.
[29] C. M. Andres, I. Larraza, T. Corrales, N. A. Kotov, *Adv. Mater.* **2012**, *24*, 4597.
[30] W. Deng, X. Zhang, C. Gong, Q. Zhang, Y. Xing, Y. Wu, X. Zhang, J. Jie, *J. Mater. Chem. C* **2014**, *2*, 1314.
[31] Y. Joo, J. Byun, N. Seong, J. Ha, H. Kim, S. Kim, T. Kim, H. Im, D. Kim, Y. Hong, *Nanoscale* **2015**, *7*, 6208.
[32] S. Niu, S. Wang, L. Lin, Y. Liu, Y. S. Zhou, Y. Hu, Z. L. Wang, *Energy Environ. Sci.* **2013**, *6*, 3576.